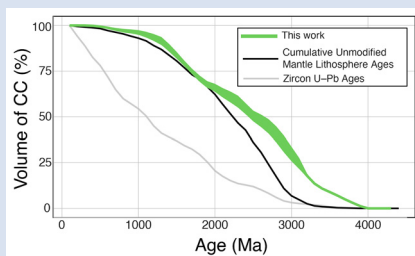


A whole-lithosphere view of continental growth

J.R. Reimink^{1*}, J.H.F.L. Davies², J.-F. Moyen³, D.G. Pearson⁴

Abstract



~2.5 Gyr of Earth history, with clear temporal links to the birth of extensive lithospheric keels and establishment of continental drainage basins.

Continental crust is a defining feature of Earth; yet, the mechanisms that control its growth remain hotly debated. Many approaches to estimating crustal growth focus solely on a single mineral—zircon, while constraints from the lithospheric mantle root remain largely neglected. Here, we critically examine the ability of zircon to accurately record the relative roles of juvenile crustal addition versus recycling, and present an alternative approach based on the geochemistry of crustal rock samples. The resulting model of continental crustal growth parallels, but pre-dates, the pattern of cratonic mantle lithosphere formation ages, indicating a distinct relationship between the continental crust and its mantle root. Our results indicate that continental crust and deep cratonic lithospheric roots grew progressively over

Received 6 June 2023 | Accepted 2 July 2023 | Published 3 August 2023

Introduction

Earth's intermediate to felsic composition continental crust is thicker and more buoyant than mafic oceanic crust, and represents an excellent archive of fundamental processes such as regulating the long-term carbon cycle, concentrating and hosting valuable mineral deposits, and providing unique habitats for biological development and diversification. Despite the importance of continental crust to humanity, there is little consensus on the timing of its formation and its stabilisation. Many widely used models, some of which are underpinned by zircon U–Pb and Hf isotope systematics (Belousova *et al.*, 2010; Dhuime *et al.*, 2012), emphasize the potential importance of voluminous continental growth in the Archean. These models produce a dramatic inflection point at ~3 Ga, where continental growth rate purportedly subsided and large tracts of crust were stabilised. However, there is little preserved evidence of this hypothesised voluminous ancient continental crust. Likewise, the continental lithospheric mantle—thick roots that stabilised ancient continental crust—have little extensive record prior to ~3.0 Ga (Pearson *et al.*, 2021).

Determining the relationship between the continental crust and the cratonic lithospheric mantle roots (CLMR) is critical in deciphering the growth of continental crust. In the modern Earth, deep lithospheric roots stabilise and appear to preserve extant continental crust (Lee *et al.*, 2017), so the discrepancy between preserved lithospheric mantle ages and previous crustal growth models (Fig. 1) suggests a genetic disconnect. Recent studies of the continental crust–CLMR relationship suggest that, while very ancient continental crust was formed and rapidly

destroyed, the formation of lithospheric roots stabilised existing continental crust, thereby slowing the destruction, and growth rate, of continents (Hawkesworth *et al.*, 2017; Pearson *et al.*, 2021). This has been taken by some authors to indicate that continental crust and continental lithospheric mantle are related by selective preservation—and that their formation mechanisms were not related (Fig. 1). However, there are considerable uncertainties in models for continental growth rates.

Destruction of an ancient crustal record can take several forms, but is typically separated into two categories (Cawood *et al.*, 2013): 1) *Reworking*—processes that overprint the radiometric ages of the crustal record, but do not remove mass from the continents, such as partial melting and sedimentary erosion, and 2) *Recycling*—full scale removal of continental mass back into the mantle by delamination or sediment and continental subduction.

While there is isotopic evidence for some amount of continental crust recycled into the modern mantle (Jackson *et al.*, 2007), there is little evidence for vast volumes of ancient continental material residing in the mantle. For instance, volatile-element isotopic measurements typically indicate the onset of detectable crustal recycling near ~2.5 Ga (Coltice *et al.*, 2000; Parai and Mukhopadhyay, 2018; Labidi *et al.*, 2020). Thus, recycling is unlikely to be a major factor in destroying large volumes of primary continental crust before 2.5 Ga. Yet, the most ancient of crust—older than ~3.8 Ga—is restricted in its exposure at the surface of the Earth to the parts per million level. Thus, if large volumes of ancient continental crust did exist on Earth, reworking must be primarily responsible for overprinting the ancient geochronological signatures of that crust. Therefore, accurate

1. Department of Geosciences, The Pennsylvania State University, University Park, PA, USA
2. Département des sciences de la Terre et de l'atmosphère/GEOTOP, Université du Québec à Montréal, Montréal, Canada
3. Laboratoire Magmas et Volcans, Université de Lyon, Saint Etienne, France
4. Department of Earth and Atmospheric Sciences, University of Alberta, AB, Canada

* Corresponding author (email: jreimink@psu.edu)

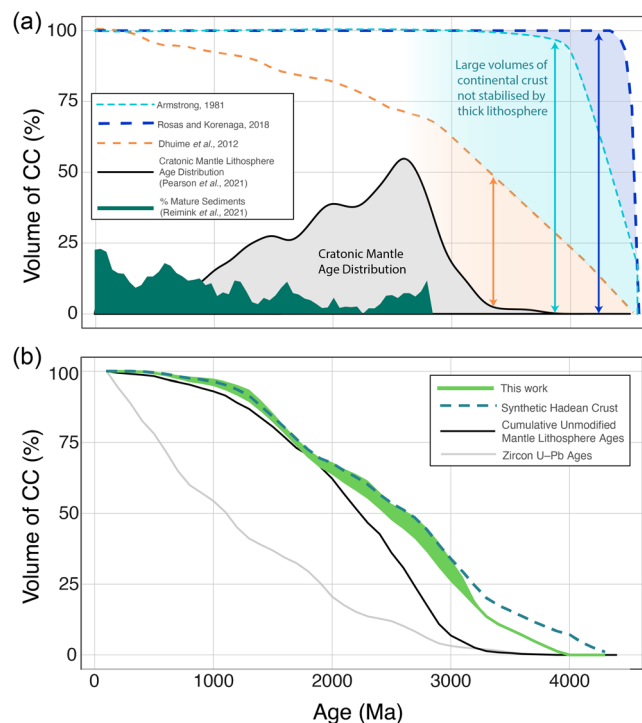


Figure 1 (a) Various crustal growth rate curves shown by dashed lines compared to the cratonic mantle age distribution. Vertical coloured arrows show the amount of continental recycling predicted by various estimates. The black curve shows the age distribution of unmodified cratonic mantle ages (Pearson et al., 2021), while the green field shows the percentage of preserved mature sedimentary packages (Reimink et al., 2021). (b) Shows the continental growth curve predicted in this work. The grey curve shows U–Pb ages of the preserved rock record (Puetz et al., 2018). The black curve is the age distribution of unmodified cratonic mantle roots (Pearson et al., 2021). The green curve is the crustal growth curve calculated here using bulk rock major element chemistry. The dashed green curve uses the same calculations as the solid green curve except for the utilisation of a synthetic Mesoarchean–Hadean rock record, to evaluate potential for sampling bias.

quantification of *reworking* is fundamentally important to model the primary formation age of continental landmasses.

Estimates of Continental Growth Rate

Recent estimates of the volumes of continental crust throughout Earth's history have relied on zircon Hf and O isotopes (Belousova et al., 2010; Dhuime et al., 2012; Korenaga, 2018). Hafnium isotopes in zircon can be used to both calculate the age of crust formation and the time the source material was extracted from the mantle, while oxygen isotope ratios have been used as a filter (Dhuime et al., 2012). Zircon oxygen isotope ratios reflect the oxygen isotope composition of the source to the zircon-forming magmas. Oxygen isotope ratios in igneous rocks can be shifted from the unaltered mantle value by incorporation of material that has interacted with surface waters, *i.e.* sediments. Such incorporation of sedimentary rocks into the igneous system, *e.g.* continental recycling, can generate zircon with high oxygen isotope ratios (Valley et al., 2005), at least on the modern Earth.

Zircon U–Pb, Hf, and O isotope data have been combined to calculate widely used crustal growth estimates (Dhuime et al., 2012) that indicate rapid crustal growth in the Archean and a

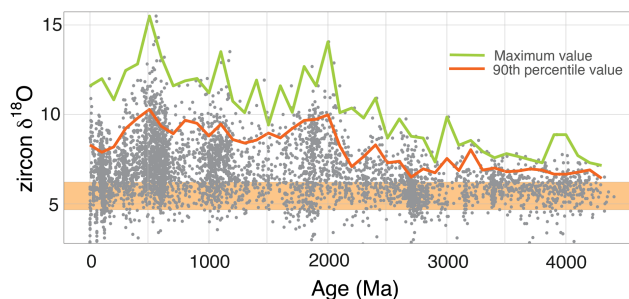


Figure 2 The distribution of zircon oxygen isotope compositions through time, highlighting the tendency of zircon oxygen isotope ratios to become progressively more extreme through time, making them a poor discriminant of continental reworking. The orange band shows a typical field for 'juvenile' zircon isotope compositions.

shift in crustal growth rate near 3.0 Ga to slower growth. Despite the popularity of this approach, drawbacks have been pointed out (Korenaga, 2018). A fundamental issue with the U–Pb/Hf/O approaches is that it is solely reliant on zircon geochemistry to accurately track continental recycling throughout geological time. While the combination of the U–Pb and Hf isotope systems may be reliable (Korenaga, 2018), the use of oxygen isotopes to track recycling is prone to uncertainty. For instance, recent studies have shown that zircon oxygen isotope ratios do not accurately identify sediment recycling in the Neoproterozoic (Bucholz and Spencer, 2019), a critical time period for constraining continental growth estimates. Additionally, the maximum oxygen isotope ratio of igneous zircons and shales (mature sedimentary rocks) continues to increase over time (Valley et al., 2005; Bindeman et al., 2018). This means that the sensitivity of the O-isotope reworking metric also changes throughout geological time (Fig. 2), making the proxy significantly less sensitive in the Archean than today. If continental reworking in the Neoproterozoic is under- or overestimated, it will impose a dramatic bias on any derivative continental growth curve.

To circumvent these issues, we take an approach that integrates the detrital zircon Hf isotope record—the record of the mantle extraction age of continental crust—with the bulk composition of the preserved continental rock record, to identify and correct for crustal reworking. We adopt this approach because the major element composition of igneous rocks can accurately quantify the extent of reworking of previous continental crust, whether reworking occurs via incorporation of sediments or direct melting of pre-existing continental crust (Frost and Frost, 2008; Moyen et al., 2017). The major-element bulk composition approach is not inherently biased towards specific rock types. Contrary to oxygen isotope ratios, the range of major element compositions of igneous rocks is limited by the thermodynamics of partial melting: by mantle melting on one side and eutectic granite melting on the other. Thus, igneous rocks have strict limits to their composition irrespective of their age, rendering them accurate and consistent tracers of continental reworking through geological time.

Crustal Reworking

Our estimate of the reworking rate of continental crust (Fig. 3) uses input from the classic ACNK/ANK diagram of Shand, (1943), further developed to isolate source composition from fractionation and assimilation trends in magmatic rocks by Moyen et al. (2017). This method is explained in detail in the Supplementary Materials. In this projection, a theta value of

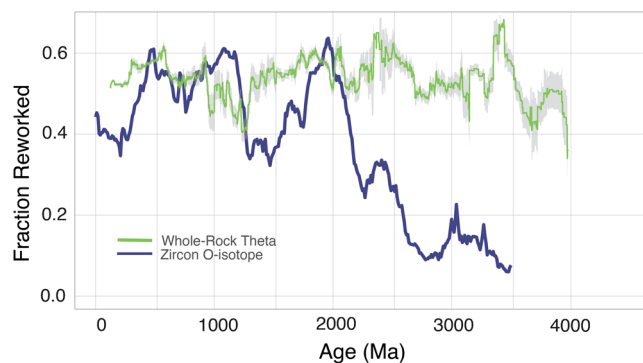


Figure 3 The fraction of rocks classified as reworked continental crust from Figure 1 using the bulk geochemistry approach adopted here (green curve with grey band showing 2SE uncertainty) compared to the reworking estimates based on zircon oxygen isotope ratios. Curves calculated in 200 Ma moving windows in 10 Ma time steps. The zircon record dramatically under-estimates reworking in the Archean.

10–30 degrees reflects crustal and peraluminous melt sources, *i.e.* a rock formed by continental reworking, whereas a theta value of less than 10 represents juvenile primitive magma with minimal crustal input (Fig. 4). An added benefit of this metric is that it classifies melts of continental crustal rocks in a similar way to melts of sedimentary rocks—useful for our purposes as both origins reflect continental reworking. This is an improvement on the commonly used aluminum saturation index, another metric used to classify whole rock geochemical data that successfully discriminates pure sediment derived melts but does not identify evolved (fractionated) compositions formed from igneous sources—a composition we must accurately identify when considering continental recycling through time.

The theta value calculation does not divide rock compositions into a binary ‘reworked’ or ‘juvenile’ category. Instead, we have employed a naïve Bayesian classifier to calculate five probabilities for each whole-rock composition, one for each class of source materials ranging from ultramafic to sedimentary. These probabilities are divided into two groups, reworked and juvenile (see Supplemental Methods for further explanation). The sum total of each reworking and juvenile probability, across all individual whole-rock measurements in any particular age bin, were then totalled to determine the reworking fraction in that age bin.

The resulting trace of crustal reworking through geological time, as viewed by the whole-rock elemental record, primarily differs from the zircon oxygen isotope record in that it is relatively constant through time. For instance, using the major element-based temporal trace in Fig. 3, the fraction of reworked crust varies by less than a factor of two (only between 0.5 and 0.3 post- 3 Ga), whereas the O-isotope based trace varies by a factor of seven, with significant swings in magnitude over short time intervals (Fig. 3).

In the Neoproterozoic, whole-rock data indicate significantly more reworking than the zircon oxygen isotope model. The causes of this difference are not readily apparent, but may be due to anoxic weathering conditions that adversely affect the ability of oxygen isotope ratios to accurately track continental reworking (Bucholz and Spencer, 2019). Many sedimentary rocks and their derivative melts are known from the Neoproterozoic period (Donaldson and de Kemp, 1998; Laurent *et al.*, 2014), indicating that continental reworking took place; yet, the existence of significant crustal reworking is not clearly captured by the zircon oxygen isotope record. The whole-rock bulk geochemical compositional record appears to be a more reliable index of crustal reworking than the zircon oxygen isotope tracer for a combination of reasons. The angular projection employed in our “reworking index”, based on major elements, can identify

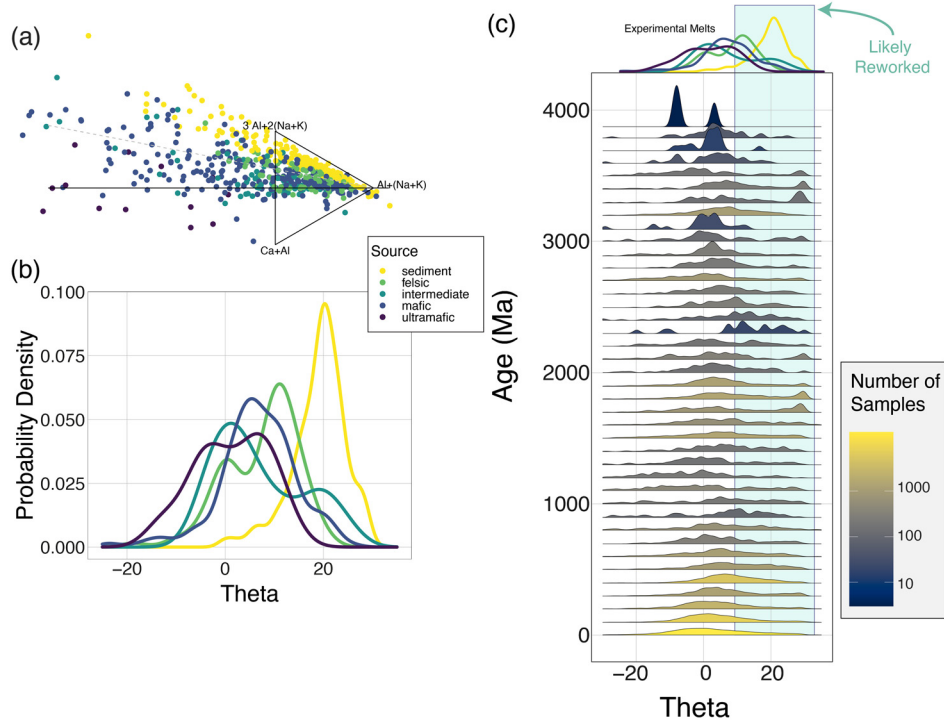


Figure 4 Reworking through time as seen through the whole-rock record. (a) The whole-rock geochemical data used to calculate a ‘theta’ value, with experimental melts shown coloured by starting composition. (b) Our classifier for data shown in panel b, showing the probability density for each category across a range of Theta values. (c) The distribution of Theta values across geological time. A probability density estimator is shown for the theta values for rocks split into 100 Ma age bins and coloured according to the number of rock samples in each age bin. Rocks that likely represent reworked crust fall into the blue field and have been present since the early Archean.

the recycling of continental igneous rocks, as well as the products of melting of sedimentary rocks—a phenomenon that zircon oxygen isotope ratios are only well-suited to detect in the post-NeoArchean rock record (Fig. 2) after large volumes of sedimentary rocks began to be deposited following continental emergence (Valley *et al.*, 2005; Reimink *et al.*, 2021).

We leverage our improved reworking metric to calculate a continental growth rate curve (Fig. 1; see [supplementary methods](#) for details) starting from a widely used crustal growth estimate based on zircon U–Pb & Hf isotopes (Dhuime *et al.*, 2012) following some refinement (Korenaga, 2018) and an updated zircon Hf dataset (Roberts and Spencer, 2015) (green curve Fig. 1b). In contrast to approaches based solely on zircon, our new bulk rock-based continental growth curve shows no slowing of continental growth at 3.0 Ga but instead indicates the onset of significant continental growth at ~3.5 Ga and reduction in crustal growth rate just before ~1.0 Ga, almost 2.0 Ga later than the zircon-based method. It has been noted that zircon Hf-isotopes have a tendency to over-estimate the mass of reworking in the source of a given rock, so the curve presented in this work (Fig. 1) likely represents a maximum crustal growth curve, as decoupling of rock mass from Hf-isotope systematics would bias the curve to artificially old ages. This over-estimation may also be a source of offset between the crust and mantle growth curves in the Mesoarchean (Fig. 1a).

The appearance of >10 % of continental crust at *ca.* 3.5 Ga coincides with a time on Earth when continental rocks were first preserved in significant volumes in the rock record. For instance, many cratonic nuclei contain rock samples that formed ~3.4–3.6 Ga (Bauer *et al.*, 2020). Thus, our calculations broadly agree with first order observations from the preserved rock record—an important test. Also, our new crustal growth curve indicates that continental growth has stagnated since ~1.1 Ga, a time on Earth marked by the appearance of preserved paired metamorphic belts (Holder *et al.*, 2019), possibly indicating the progressive evolution of plate tectonics to a modern style of colder and steeper subduction. This timing coincides with a dramatic slowing of new additions to cratonic mantle lithosphere (Pearson *et al.*, 2021), pointing to a shared lineage between stable crust and mantle lithosphere. Note that we have performed key sensitivity tests on our modelling results (preservational bias, chemical biases, *etc*) that show that our crustal growth rate curves are immune to systematic biases (Figs. S7–9).

Crustal Growth Rates

The continental growth rate reflected in global bulk rock data suggests a temporal relationship between the evolution of continental crust and the formation of deep, stable sub-continental lithospheric mantle roots that are key to defining the cratons. This relationship is very different to that previously proposed based on alternative continental growth curves (Dhuime *et al.*, 2012; Korenaga, 2018) which argue for a preservational relationship between continental crust and deep mantle roots (Hawkesworth *et al.*, 2017; Pearson *et al.*, 2021), whereby large volumes of deep mantle keels stabilised and preserved extant continental crust, whereas older, unstabilised continental crust was preferentially reworked. Instead, our bulk rock-based estimate of continental growth indicates that continental crust and deep mantle keels may have been formed in a similar time window, with the key inflection point being at ~1 Ga, a defining point for cratons (Pearson *et al.*, 2021). Continental crust begins to grow prior to the mantle lithosphere as recorded in mantle xenoliths on the modern Earth. The difference in growth rate could be due to mantle lithosphere being overprinted by younger magmatic events (Pearson *et al.*, 2002; Alard *et al.*, 2005; Liu *et al.*,

2021). This may be likely as >2.85 Ga diamond-bearing lithosphere clearly exists in several cratonic regions (Smart *et al.*, 2016; Timmerman *et al.*, 2022). Thus, we emphasise that any mechanism proposed to explain either the formation of ancient continental crust or their underlying deep mantle keels, features that collectively define the cratons (Pearson *et al.*, 2021), must account for the formation of both features at nearly the same time (Pearson *et al.*, 2007). The inflection in continental growth began near 3.5 Ga and has substantially slowed since ~1.0 Ga (Fig. 1), a feature mirrored by continental roots (Pearson *et al.*, 2021). Though felsic crust clearly cannot be derived directly from peridotite, this broad temporal link points to the possibility of mechanistic links in the formation of continental crust and the rapid docking of thick lithospheric keels beneath them, perhaps by lateral accretion and slab imbrication—a process that has been separately invoked for the production of ancient continental crust (Bauer *et al.*, 2020) and ancient lithospheric mantle (Timmerman *et al.*, 2022).

Our continental growth curve indicates that Earth's volumes of continental crust grew progressively over a 2.5 Gyr period in the middle of Earth history. There is no evidence for either large volumes of Hadean continental crust, nor signs of a decrease in crustal growth rate near 3.0 Ga, removing a key constraint used to argue for a geodynamic shift in Earth's tectonic regime near that time. Instead, our analysis indicates that most continental crust grew between 3.5 Ga and *ca.* 1.0 Ga in a relatively consistent manner (Condie *et al.*, 2018; Garçon, 2021), occurring over the same time period that cratonic mantle roots formed (Pearson *et al.*, 2021). Though the links between continental growth, craton root development, and the emergence of freeboard remain to be fully understood, our analysis suggests that they may be unrelated to a distinct change in the geodynamics of the solid Earth in the Neoproterozoic. Instead, our analysis places emphasis on the change in lithosphere evolution in the Mesoarchean, and may suggest that continental freeboard on Earth formed simply due to continent formation in large volumes (Reimink *et al.*, 2021). Thus, continental emergence and the rise of subaerial weathering cycles may have been caused simply by the formation and stabilisation of the continents themselves.

Data Availability

The data reduction code used to process this data set can be found in the [Supplementary Information](#). Zircon U–Pb data shown in Figure 1 is from Puetz and Condie, (2019).

Acknowledgements

Roberta Rudnick and an anonymous reviewer are thanked for their comments that led to substantial improvements in this manuscript. Ambre Luguët and Raúl Fonseca are thanked for their comments and editorial handling in the production of this publication.

Editor: Ambre Luguët and Raúl Fonseca

Additional Information

Supplementary Information accompanies this letter at <https://www.geochemicalperspectivesletters.org/article2324>.



© 2023 The Authors. This work is distributed under the Creative Commons Attribution 4.0 License, which permits unrestricted use,

distribution, and reproduction in any medium, provided the original author and source are credited. Additional information is available at <http://www.geochemicalperspectivesletters.org/copyright-and-permissions>.

Cite this letter as: Reimink, J.R., Davies, J.H.F.L., Moyen, J.-F., Pearson, D.G. (2023) A whole-lithosphere view of continental growth. *Geochem. Persp. Let.* 26, 45–49. <https://doi.org/10.7185/geochemlet.2324>

References

- ALARD, O., LUGUET, A., PEARSON, N.J., GRIFFIN, W.L., LORAND, J.-P., GANNOUN, A., BURTON, K.W., O'REILLY, S.Y. (2005) In situ Os isotopes in abyssal peridotites bridge the isotopic gap between MORBs and their source mantle. *Nature* 436, 1005–1008. <https://doi.org/10.1038/nature03902>
- BAUER, A.B., REIMINK, J.R., CHACKO, T., FOLEY, B.J., SHIREY, S.B., PEARSON, D.G. (2020) Hafnium isotopes in zircons document the gradual onset of mobile-lid tectonics. *Geochemical Perspectives Letters* 14, 1–6. <https://doi.org/10.7185/geochemlet.2015>
- BELOUSOVA, E.A., KOSTITSYN, Y.A., GRIFFIN, W.L., BEGG, G.C., O'REILLY, S.Y., PEARSON, N.J. (2010) The growth of the continental crust: Constraints from zircon Hf-isotope data. *Lithos* 119, 457–466. <https://doi.org/10.1016/j.lithos.2010.07.024>
- BINDEMAN, I.N., ZAKHAROV, D.O., PALANDRI, J., GREBER, N.D., DAUPHAS, N., RETALLACK, G.J., HOFMANN, A., LACKEY, J.S., BEKKER, A. (2018) Rapid emergence of subaerial landmasses and onset of a modern hydrologic cycle 2.5 billion years ago. *Nature* 557, 545–548. <https://doi.org/10.1038/s41586-018-0131-1>
- BUCHOLZ, C.E., SPENCER, C.J. (2019) Strongly Peraluminous Granites across the Archean–Proterozoic Transition. *Journal of Petrology* 60, 1299–1348. <https://doi.org/10.1093/ptrology/egz033>
- CAWOOD, P.A., HAWKESWORTH, C.J., DHUIME, B. (2013) The continental record and the generation of continental crust. *Geological Society of America Bulletin* 125, 14–32. <https://doi.org/10.1130/B30722.1>
- COLTICE, N., ALBARÈDE, F., GILLET, P. (2000) ^{40}K - ^{40}Ar Constraints on Recycling Continental Crust into the Mantle. *Science* 288, 845–847. <https://doi.org/10.1126/science.288.5467.845>
- CONDIE, K.C., PUETZ, S.J., DAVAILLE, A. (2018) Episodic crustal production before 2.7 Ga. *Precambrian Research* 312, 16–22. <https://doi.org/10.1016/j.precamres.2018.05.005>
- DHUIME, B., HAWKESWORTH, C.J., CAWOOD, P.A., STOREY, C.D. (2012) A Change in the Geodynamics of Continental Growth 3 Billion Years Ago. *Science* 335, 1334–1336. <https://doi.org/10.1126/science.1216066>
- DONALDSON, J.A., DE KEMP, E.A. (1998) Archean quartz arenites in the Canadian Shield: examples from the Superior and Churchill Provinces. *Sedimentary Geology* 120, 153–176. [https://doi.org/10.1016/S0037-0738\(98\)00031-1](https://doi.org/10.1016/S0037-0738(98)00031-1)
- FROST, B.R., FROST, C.D. (2008) A Geochemical Classification for Feldspathic Igneous Rocks. *Journal of Petrology* 49, 1955–1969. <https://doi.org/10.1093/ptrology/egn054>
- GARÇON, M. (2021) Episodic growth of felsic continents in the past 3.7 Ga. *Science Advances* 7, eabj180. <https://doi.org/10.1126/sciadv.abj1807>
- HAWKESWORTH, C.J., CAWOOD, P.A., DHUIME, B., KEMP, T.I.S. (2017) Earth's Continental Lithosphere Through Time. *Annual Review of Earth and Planetary Sciences* 45, 169–198. <https://doi.org/10.1146/annurev-earth-063016-020525>
- HOLDER, R.M., VIETE, D.R., BROWN, M., JOHNSON, T.E. (2019) Metamorphism and the evolution of plate tectonics. *Nature* 572, 378–381. <https://doi.org/10.1038/s41586-019-1462-2>
- JACKSON, M.G., HART, S.R., KOPPERS, A.A.P., STAUDIGEL, H., KONTER, J., BLUSZTAJN, J., KURZ, M., RUSSELL, J.A. (2007) The return of subducted continental crust in Samoan lavas. *Nature* 448, 684–687. <https://doi.org/10.1038/nature06048>
- KORENAGA, J. (2018) Estimating the formation age distribution of continental crust by unmixing zircon ages. *Earth and Planetary Science Letters* 482, 388–395. <https://doi.org/10.1016/j.epsl.2017.11.039>
- LABIDI, J., BARRY, P.H., BEKAERT, D.V., BROADLEY, M.W., MARTY, B., GIUNTA, T., WARR, O., SHERWOOD LOLLAR, B., FISCHER, T.P., AVICE, G. and CARACASI, A. (2020) Hydrothermal ^{15}N abundances constrain the origins of mantle nitrogen. *Nature* 580, 367–371. <https://doi.org/10.1038/s41586-020-2173-4>
- LAURENT, O., MARTIN, H., MARTIN, H., MOYEN, J.F., MOYEN, J.-F., DOUCELANCE, R., DOUCELANCE, R. (2014) The diversity and evolution of late-Archean granitoids: Evidence for the onset of “modern-style” plate tectonics between 3.0 and 2.5Ga. *Lithos* 205, 1–82. <https://doi.org/10.1016/j.lithos.2014.06.012>
- LEE, C.-T.A., CAVES, J., JIANG, H., CAO, W., LENARDIC, A., MCKENZIE, N.R., SHORTLE, O., YIN, Q., DYER, B. (2017) Deep mantle roots and continental emergence: implications for whole-Earth elemental cycling, long-term climate, and the Cambrian explosion. *International Geology Review* 60, 1–18. <https://doi.org/10.1080/00206814.2017.1340853>
- LIU, J., PEARSON, D.G., WANG, L.H., MATHER, K.A., KJARSGAARD, B.A., SCHAEFFER, A.J., IRVINE, G.J., KOPYLOVA, M.G., ARMSTRONG, J.P. (2021) Plume-driven re-creation of deep continental lithospheric mantle. *Nature* 592, 732–736. <https://doi.org/10.1038/s41586-021-03395-5>
- MOYEN, J.-F., LAURENT, O., CHELLE-MICHOU, C., COUZINIÉ, S., VANDERHAEGHE, O., ZEH, A., VILLAROS, A., GARDIEN, V. (2017) Collision vs. subduction-related magmatism: Two contrasting ways of granite formation and implications for crustal growth. *Lithos* 277, 154–177. <https://doi.org/10.1016/j.lithos.2016.09.018>
- PARAI, R., MUKHOPADHYAY, S. (2018) Xenon isotopic constraints on the history of volatile recycling into the mantle. *Nature* 560, 223–227. <https://doi.org/10.1038/s41586-018-0388-4>
- PEARSON, D.G., PARMAN, S.W., NOWELL, G.M. (2007) A link between large mantle melting events and continent growth seen in osmium isotopes. *Nature* 449, 202–205. <https://doi.org/10.1038/nature06122>
- PEARSON, D.G., SCOTT, J.M., LIU, J., SCHAEFFER, A., WANG, L.H., VAN HUNEN, J., SZILAS, K., CHACKO, T., KELEMEN, P.B. (2021) Deep continental roots and cratons. *Nature* 596, 199–210. <https://doi.org/10.1038/s41586-021-03600-5>
- PEARSON, N.J., ALARD, O., GRIFFIN, W.L., JACKSON, S.E., O'REILLY, S.Y. (2002) In situ measurement of Re-Os isotopes in mantle sulfides by laser ablation multicollector-inductively coupled plasma mass spectrometry: analytical methods and preliminary results. *Geochimica et Cosmochimica Acta* 66, 1037–1050. [https://doi.org/10.1016/S0016-7037\(01\)00823-7](https://doi.org/10.1016/S0016-7037(01)00823-7)
- PUETZ, S.J., CONDIE, K.C. (2019) Time series analysis of mantle cycles Part I: Periodicities and correlations among seven global isotopic databases. *Geoscience Frontiers* 10, 1305–1326. <https://doi.org/10.1016/j.gsf.2019.04.002>
- REIMINK, J.R., DAVIES, J.H.F.L., IELPI, A. (2021) Global zircon analysis records a gradual rise of continental crust throughout the Neoproterozoic. *Earth and Planetary Science Letters* 554, 116654. <https://doi.org/10.1016/j.epsl.2020.116654>
- ROBERTS, N.M.W., SPENCER, C.J. (2015) The zircon archive of continent formation through time. *Geological Society, London, Special Publications* 389, 197–225. <https://doi.org/10.1144/SP389.14>
- SHAND, S.J. (1943) *Eruptive rocks: their genesis, composition, and classification, with a chapter on meteorites*. J. Wiley & sons, Incorporated.
- SMART, K.A., TAPPE, S., STERN, R.A., WEBB, S.J., ASHWAL, L.D. (2016) Early Archean tectonics and mantle redox recorded in Witwatersrand diamonds. *Nature Geoscience* 9, 1–6. <https://doi.org/10.1038/ngeo2628>
- TIMMERMAN, S., REIMINK, J.R., VEZINET, A., NESTOLA, F., KUBLIK, K., BANAS, A., STACHEL, T., STERN, R.A., LUO, Y., SARKAR, C. and IELPI, A. (2022) Mesoarchean diamonds formed in thickened lithosphere, caused by slab-stacking. *Earth and Planetary Science Letters* 592, 117633. <https://doi.org/10.1016/j.epsl.2022.117633>
- VALLEY, J.W., LACKEY, J.S., CAVOSIE, A.J., CLECHENKO, C.C., SPICUZZA, M.J., BASEI, M.A.S., BINDEMAN, I.N., FERREIRA, V.P., SIAL, A.N., KING, E.M., PECK, W.H., SINHA, A.K. and WEI, C.S. (2005) 4.4 billion years of crustal maturation: oxygen isotope ratios of magmatic zircon. *Contributions to Mineralogy and Petrology* 150, 561–580. <https://doi.org/10.1007/s00410-005-0025-8>



A whole-lithosphere view of continental growth

J.R. Reimink, J.H.F.L. Davies, J.-F. Moyen, D.G. Pearson

Supplementary Information

The Supplementary Information includes:

- Methods
- Tables S-1 to S-4
- Figures S-1 to S-11
- Supplementary Information References

Methods

Previous Crustal Growth Estimates

Previous crustal growth estimates calculated by Dhuime *et al.*, (2012; 2017) are here collectively referred to as D27 and these widely used crustal growth curves are based on a modification of the calculations of Belusova *et al.* (2010). In the calculation scheme used by D27, an age spectrum was obtained by compiling zircon Hf-isotope depleted mantle model extraction ages. Each individual zircon U-Pb + Hf isotope data point was used to calculate a depleted mantle model extraction age, and these model ages were binned across geologic time. This age distribution was corrected for reworking using a modification of the methods employed by (Belousova *et al.*, 2010). Instead of considering only zircon Hf isotope data, D27 used zircon O-isotope data to identify crustal reworking signals in the zircon record where zircon oxygen isotope values above the mantle range were considered to be evidence of a reworking signal. A curve proposed to be the crustal growth rate was calculated by determining the relationship between crustal reworking – identified using zircon Hf isotope model ages – and juvenile crustal growth – identified using O-isotope ratios. These calculations are replicated in Supplementary Table S-2. However, there is a flaw in the calculations employed in the D27 work (as pointed out by (Korenaga, 2018)).

The New Crust Generation Rate in the original formulation is calculated by

$$100 - \text{Crustal Reworking Rate.}$$

The Crustal Reworking Rate was calculated by taking:

$$100 * (\text{Reworked Crust Ages} / (\text{Reworked Crust Ages} + \text{Calculated New Crustal Ages}))$$



As this equation shows, the derived value is a ratio of ages, and is therefore non-dimensional (Korenaga, 2018). Thus, the Crustal Reworking Rate value is not in fact a rate, but a ratio of reworked crust / all crust, and likewise the New Crust Generation Rate is not a rate but a ratio of New Crust to Total Crust. These ratios, which by definition must be between 0-1 (or 0-100 when multiplied by 100), cannot be summed over time in a meaningful way; performing a cumulative sum calculation on non-dimensional values between 0-100 is meaningless.

This is best understood when considering a hypothetical example. If 1,000 zircons are formed between 1000-1100 Ma, and 10,000 zircons are formed between 1100-1200 Ma, the goal is to determine how many juvenile zircons formed between 1000 and 1200 Ma. The first step is to determine how many zircons derived from reworked crust and how many formed from juvenile crust. This can be determined by taking the ratio of Reworked Crust / Total Crust, or the number of zircons formed from reworked sources / total number of zircons. Hypothetically assuming that the reworking ratio is 50% in each time interval. To calculate the crustal growth rate, or the cumulative number of juvenile crust ages through time, the cumulative total of the 50% reworking ratio should be multiplied back onto the age distribution to get 500 juvenile zircons between 1000-1100 Ma and 5,000 between 1100-1200 Ma. These zircon ages should be cumulatively summed over this time interval to calculate a juvenile growth rate. Thus, the derived ratios of New Crust/Total Crust must be applied to an age distribution to get cumulative juvenile ages through time, which then can be cumulatively summed to get a growth curve through time. If not, the ratio is just the relative proportion of new crust to reworked crust over time, not the amount of new crust.

Our crustal growth estimate

We take an approach that modifies the D27 calculation by applying a New Crust Generation (Rate) value – the ratio of new crust to total crust at any given time interval – and multiplying this value back onto the age distribution of zircon Hf-isotope depleted mantle model ages. These values, now juvenile zircon ages per time interval, are cumulatively summed through Earth history to yield a model crustal growth rate based on zircon Hf data corrected for crustal reworking using zircon O-isotope data (Fig. S-1). It is important to note that this crustal growth calculation is still underpinned by the Hf-isotope model age distribution, so the method does not solely rely on the major element composition of granitoids or zircon oxygen isotopes through time.



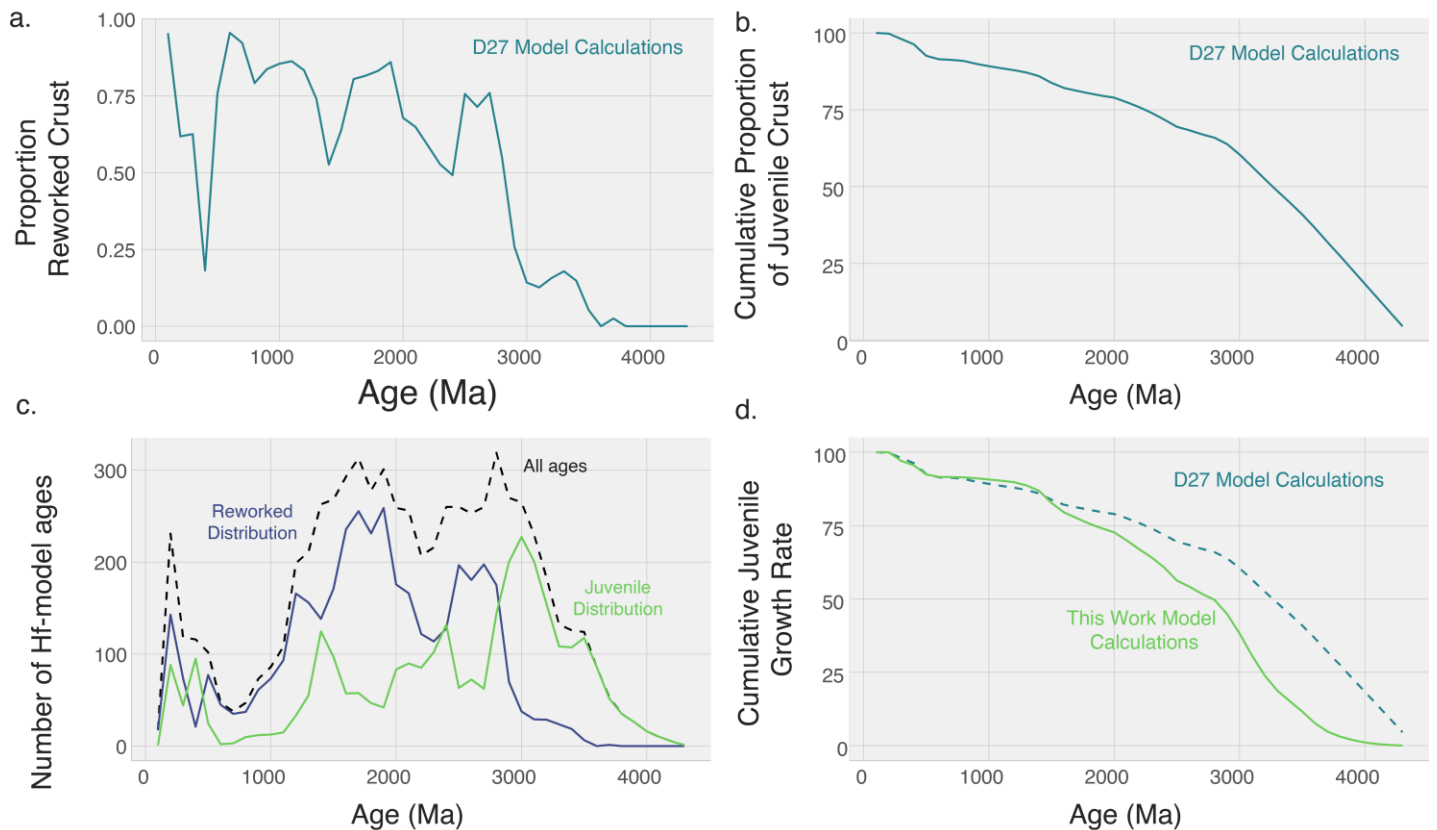


Figure S-1 A figure reproducing the calculations of Dhuime *et al.* (2012) illustrating the error in those calculations. **(a)** Shows the proportion of reworked crust / total crust in each age bin (called Crustal Reworking Rate by Dhuime *et al.*, 2012). This is a ratio of reworked to total crust and is therefore limited at 1 – or 100 when multiplied to get a percent. The inverse of this reworking ratio, the ratio of juvenile crust / total crust, was then cumulatively summed to get the curve shown in **(b)**, **(b)** Shows the cumulative proportion of juvenile crust, not a crustal growth rate. To get an actual growth rate, the proportion of juvenile crust must be multiplied back onto a real age distribution, as done in the bottom panels (c and d). **(c)** Shows the Hf model age distribution from Dhuime *et al.*, (2012) in the black dashed curve. The proportion reworked and proportion juvenile (derived from the top left curve) is multiplied onto this age distribution curve to get the number of reworked and juvenile ages in each age bin. This value can then be summed through geological time to get a cumulative juvenile growth rate – the green curve shown in **(d)**. **(d)** Shows the cumulative proportion curve (which is published as a growth rate in D27) as the dashed line to highlight the dramatic difference between the two calculations. Our analysis uses the framework outlined in the lower panels (c and d) using a more recently updated database of Hf model ages (Roberts and Spencer, 2015) and uses whole rock elemental variations instead of less reliable zircon O-isotope ratios to track reworking.

Errors in Quantification of Continental Reworking using Zircon O-isotopes

As discussed in the main text, zircon oxygen isotope ratios are not ideal tracers of crustal reworking. We expand our rationale for this statement here. Two primary reasons cast doubt on the veracity of O isotopes as faithful recorders of reworking 1) the maximum $\delta^{18}\text{O}$ value of zircons continue to increase throughout geologic time, and 2) Archean zircon $\delta^{18}\text{O}$ values are very limited in range. This combination means that any continental reworking filter based on zircon oxygen isotope ratios does not scale linearly across geologic time



and provides a biased view on crustal reworking. For instance, ongoing crustal reworking in the Archean – detected in the whole rock record (Bucholz and Spencer, 2019; Laurent *et al.*, 2014) and potentially in the ancient zircon record (Ackerson *et al.*, 2021) – is not readily obvious in the zircon O-isotope record.

There may be several reasons for this. First, when considering strongly peraluminous granites (SPGs) derived from nearly pure sediment melting (a classic example of continental reworking) Bucholz and Spencer (2019) show that the source clay mineral content incorporated into SPGs is nearly identical across the Archean-Proterozoic boundary despite a difference in zircon oxygen isotope ratios within the same sample suite. This indicates that oxygen isotopes in these rocks are not tracing a change in the amount of recycled component in the melt. The Bucholz and Spencer (2019) result may be due to variable oxidation states experienced by the sediments prior to melting to form the SPGs as they formed before and after the oxygenation of Earth's atmosphere. Also, Archean sedimentary rocks have been shown to have a more subdued oxygen isotope composition than Phanerozoic sedimentary rocks (Bindeman *et al.*, 2016), potentially related to maturation of the continental crust and the weathering cycle throughout geologic time. Thus, even if the oxygen isotope composition of Archean S-type granites behaved in an identical manner to the modern, the limited range in shale oxygen isotope values would limit the ability of zircon oxygen isotopes to detect reworking.

Another possible issue is that continental reworking is not only generated by sedimentary melting but can also be caused by direct melting of continental igneous rocks. While this process (essentially magmatic differentiation) can shift oxygen isotope ratios in magmatic zircons slightly above the mantle field (Bucholz *et al.*, 2017), it is unlikely to produce zircons with oxygen isotope ratios that are dramatically higher than the mantle composition. Such continental igneous recycling is likely to occur in higher proportions in the Archean Earth, and be potentially undetected by oxygen isotopes in zircon, especially if continental crust was mostly submerged beneath oceans (Bindeman *et al.*, 2018; Dong *et al.*, 2021; Kump and Barley, 2007; Reimink *et al.*, 2021) and did not produce sediments at a similar rate to the modern world.

Thus, zircon oxygen isotope ratios are not accurate trackers of continental reworking throughout Earth history. Zircons formed in magmas derived from continental reworking, in this case in the form of melting sedimentary rocks, are more likely to have subdued oxygen isotope compositions, especially in older samples. This means that a reworking filter based on zircon oxygen isotopes is unreliable and should not be used to assess the relative roles of growth versus re-working through geological time.

Calculating crustal reworking using zircon oxygen isotopes will bias any crustal growth records to artificially rapid early growth rates, particularly in the Archean. For instance, if continental reworking did occur in the Neoproterozoic (2.5-3.2 Ga), but zircon oxygen isotopes recorded no continental reworking, all ages in the Neoproterozoic would be classified as juvenile additions to the continental crust.

Tracking Continental Reworking Using the Whole Rock Major Element Compositional Record

The very extensive whole-rock major element compositional record suffers from fewer biases than the zircon oxygen isotope record as a potential tracer of continental reworking. First, there are petrologically imposed limits to the compositional endmembers that occur on Earth. The eutectic granite minimum defines one compositional limit (for most igneous rocks) and the pressure/temperature regimes in the mantle limit the types of magmas produced by partial melting of peridotite. While there is a time-dependency to the latter – for instance komatiite magmas were much more prevalent in the Archean than today (Arndt *et al.*, 2008; Grove and Parman, 2004; Walter, 1998) and sodic granitoids made up a larger fraction of the Archean continental crust than today (Martin, 1986; Moyen and Martin, 2012) – the compositional endmembers have largely



remained fixed. This means that discrete reworking indices will be time-invariant and can be reliably applied across the geologic record. Second, unlike zircons, which are limited in their occurrence to rock-types that have suitable silica activities and alkalinities to crystallise them, the whole rock record is not restricted to a particular end of the rock spectrum. This suggests that using the major element composition of continental rocks may provide a better path to defining reworking through geologic time, assuming that the exposed continental crust is broadly representative of the spectrum of rock compositions at any given time – an assumption implicit in any approach, whether mineralogical or bulk rock, that uses exposed crustal rocks to track continental reworking.

Classic indicators of the melting of sediments, one form of continental reworking, include the aluminum saturation index (ASI), which is similar in function to the classic A/CNK index of (Shand, 1943). The ASI index separates metaluminous from peraluminous melts, and has been used to differentiate granites formed by partial melting of sedimentary rocks, so-called S-type granites, from those derived from melting of igneous protoliths, I-type granites (Chappell and White, 2001; Frost *et al.*, 2001). However, rocks with elevated ASI values can be produced by fractional crystallization of melts formed from melting of igneous protoliths (Frost *et al.*, 2001), while peraluminous melts can contain a mixture of mantle and crustal sources (Collins, 1996; Gray, 1984; Kemp *et al.*, 2007).

To avoid the complexities associated with the ASI classification, Moyen *et al.* (2017) derived a projection that can isolate compositional diversification driven by fractionation versus source variability. The details of this plotting scheme can be found in the supplements to Moyen *et al.* (2017) and (Bonin *et al.*, 2020) but are summarised here briefly. Essentially, the plotting relies on an expansion of the ‘closed Shand diagram’ to be plotted from biotite compositions and expanded to show more compositional diversity (Figure S-2). This plot results in an open ternary diagram (where compositions can plot outside the ternary boundaries) that has Al+(Na+K) on one apex, Ca+Al on another, and 3Al+2Na+K on the last. In this space, the A/CNK link runs perpendicular to the Al+(Na+K) apex. To further understand the validity of this plotting projection, Moyen *et al.* (2017) plotted the melt compositions from experimental partial melting reactions, coloured by the starting material composition.

Figure S-2 shows how the Theta parameter is calculated from a whole-rock major element composition. The Theta value (or angle from the horizontal) is very similar to the “alpha” parameter derived in Bonin *et al.* (2020), where a theta value of zero plots along the horizontal A/CNK=1 line. In this plotting space, Moyen *et al.* (2017) showed that experimentally derived melt compositions do not cluster but instead create linear arrays (Figure S-3). Melts derived from sedimentary starting compositions are clearly differentiated from partial melts of mafic rocks. Importantly for our purposes, melts created from felsic crustal sources, an important source of continental reworking that is not captured by the peraluminous/metaluminous definition, can be distinguished from partial melts of mafic (and ultramafic) sources.



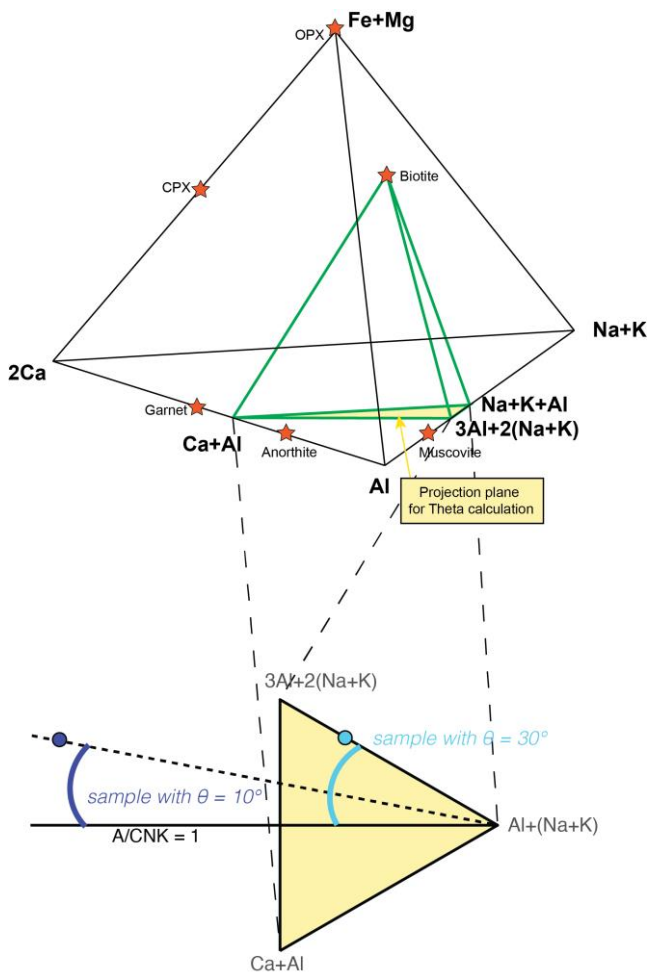


Figure S-2 Representation of the bulk rock major element plotting scheme derived by Moyen *et al.* (2017). The lower yellow triangle shows how the Theta value is calculated, where the blue data point has a theta value of 30 and the purple rock composition has a theta value of 10. A theta of 0 plots along the horizontal A/CNK=1 line. This derivation is very similar to the ‘alpha’ metric derived in Bonin *et al.* (2020).

Using the distribution of melts produced during partial melting experiments, derived from different starting source compositions, we designed a simple naïve Bayesian classifier to determine the probability that any given rock composition is produced by partial melting of a given source composition. Figure S-3 shows a schematic diagram and example calculation of our Bayesian classifier. Figure S-3a shows the distribution of experimental partial melt compositions, coloured by the starting composition. Figure S-3b shows the kernel density estimate of the theta values for melts generated from each bulk composition. Melts from sedimentary bulk compositions (in yellow) have a peak at 20° theta, while ultramafic compositions (dark purple) have a double peak at ~5° and ~-5°. Fig. S-3b also shows the calculated probability that a rock with Theta=11° (red

vertical line, and dashed line in Fig S-3a) was sourced from each bulk compositional category (horizontal coloured lines with probabilities labeled). Figure S-3c shows a table with the raw probabilities for that same rock with Theta=11°, matching the measurements from the y-axis in Figure S-3b. These probabilities are then normalised to the total probability density for that particular rock, and relative probabilities are calculated. Thus, in our calculation, a rock with theta = 11° has an ~8% chance of being derived from a sediment, ~35% chance of being derived from a felsic source, ~12% chance of being sourced from an intermediate rock, ~26% from a mafic source, and ~17% from an ultramafic source. In this way, we apply probabilities to each individual rock composition, which allows us to estimate the source composition while considering the scatter of the experimental melt compositional data.

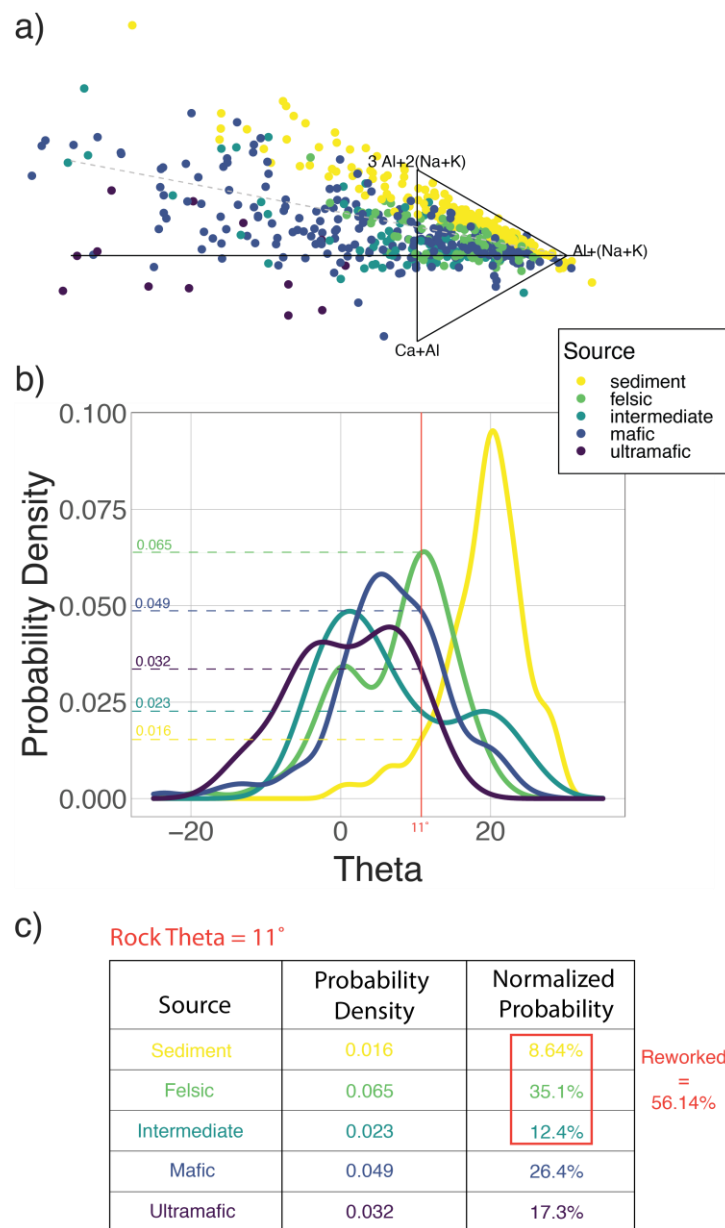


Figure S-3 Schematic illustration of the naïve Bayesian classifier derived here to estimate the probability any given rock was derived from one of five source categories, based on the compositional plotting derived by Moyen *et al.* (2017) and Bonin *et al.* (2020). See text for a detailed explanation. **(a)** Shows the experimental data compiled in Moyen *et al.* (2017) colored by source composition. **(b)** Shows the distribution of theta values of the experimental compositions shown in (a), broken apart by source composition, and **(c)** shows the source composition probability estimate breakdown, based on the theta values, for an example rock with a theta value of 11.

Using this naïve Bayesian classifier, we then simplify the five categories down to two – reworked and juvenile. For this analysis, we are simply attempting to determine the probability a given rock represents reworked continental crust. To do this, we sum up the probability in the sedimentary, felsic, and intermediate source categories. The remaining percentage is the probability a given rock is from a juvenile source. Figure S-4

shows the breakdown of probability density and normalised probability for rock compositions across a range of theta values.

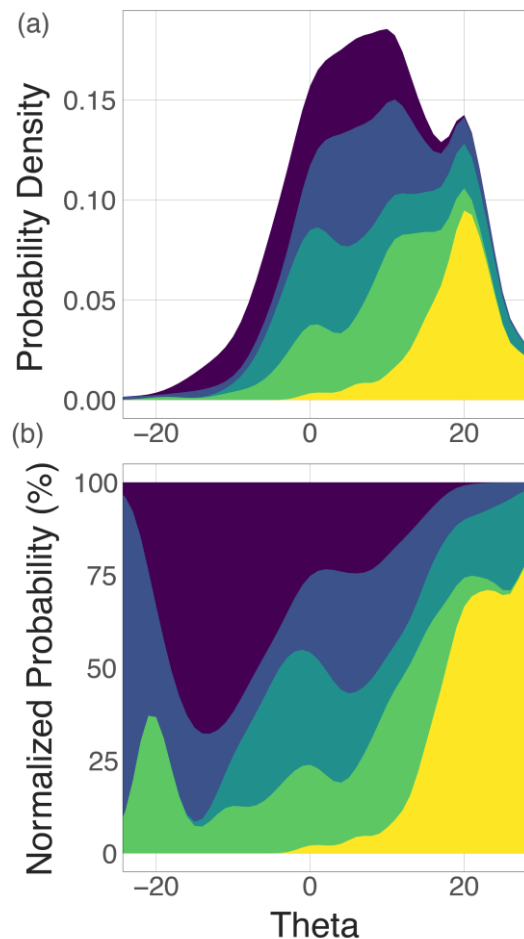


Figure S-4 Probabilities output from our naïve Bayesian classifier for a range of rock theta values. **(a)** Shows the raw probability density across the theta values, and **(b)** shows the normalised probability, in percent, for each theta value.

Moyen *et al.* (2017) showed that rocks from the French Massif Central (FMC) generally have highly positive theta values (following the terminology we use here). Figure S-5 shows the results of our calculations for both the FMC samples and those from the Kohistan Arc Batholith (Jagoutz, 2014). Our probability-based calculation assigns high probability to the FMC suite sample being reworked, with the Kohistan Arc Batholith being significantly less likely to be derived from reworking of pre-existing felsic crust. While our model suggests that there is some probability that individual Kohistan rocks may represent reworking, there exists a substantial difference between the probability of reworking for these rocks compared to FMC suite rocks (Fig. S-5). Additionally, as discussed below, systematic offsets in reworking will not substantially modify our crustal growth rate calculations – only age-varying errors will change this.

Therefore, to calculate reworking probabilities, igneous whole rock data must be compared to the experimental database shown by Moyen *et al.* (2017). We have done this for each sample in the (Gard *et al.*, 2019) igneous rock compilation, and then determined the probability of reworking for each sample.

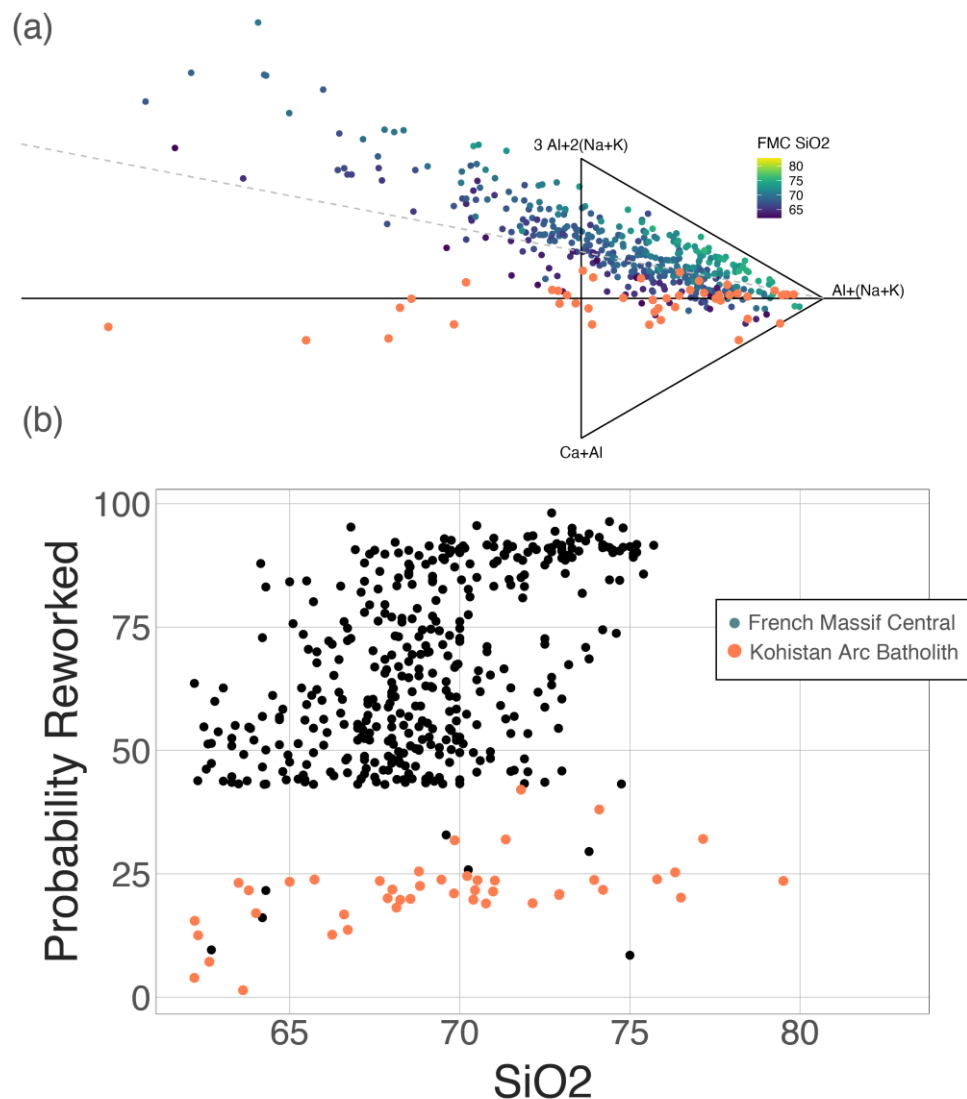


Figure S-5 Whole-rock data from the French Massif Central from Moyen *et al.* (2017, as well as Kohistan Batholith samples plotted in the theta compositional framework in (a) and shown with each samples calculated probability of being reworked crust in (b). Igneous rocks from the French Massif Central were formed by reworking of continental crust, while the Kohistan Arc Batholith was formed in a juvenile arc environment derived from juvenile mantle melts (Jagoutz, 2014). The data shown in this plot are from Moyen *et al.* (2017) and references are found in that work; the FMC data points in (a) are coloured according to their SiO_2 content while those in (b) are black, due to SiO_2 being shown in the x-axis.

We then calculate the proportion of re-worked crust in 100 Ma age bins (Figs. 1-2) by calculating the ratio of reworked/juvenile rock types within each age interval. The proportion of juvenile rocks through time is shown in Fig. 2 as a moving average, calculated in 250 Ma moving windows in 25 Ma increments. The database used for these calculations is accessible as Supplementary Table S-1. We also plot the difference between our theta metric and the ASI values calculated for each rock (Fig. S-6), which shows that in general samples with theta values between 10 and 30 (here considered to represented re-worked sources) have high ASI, but not universally. The correlation is not perfect, because these theta values may be produced by melting of igneous sources rather than sediments, which is also a crustal re-working process.

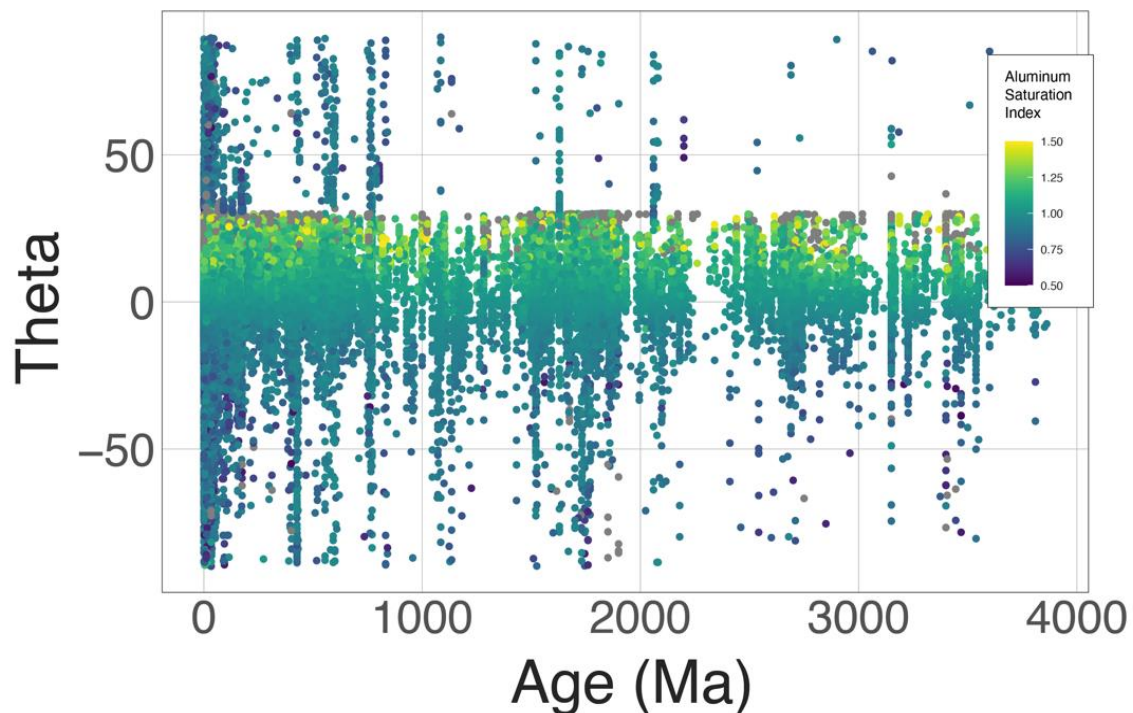


Figure S-6 The whole rock igneous database (Gard *et al.*, 2019), filtered for $\text{SiO}_2 > 62$ wt.%, and filtered for samples with complete major element data. The symbols are coloured for their ASI value, and the correlation between Thetas of 10-30 and relatively high ASI values can be seen. Note that not all rocks with theta between 10-30 degrees have high ASI values as melting of felsic igneous material also yields a theta value in this range, without producing a rock with high ASI, though these melting products still represent reworking of continental material. Theta values >30 wrap around the plotting space and there is a smooth transition from Theta = 90 to Theta = -90.

To calculate the reworking fraction through time shown in Figure 2 of the manuscript, we performed the following calculation. First, the normalised probabilities for each of the five source categories was calculated for each rock composition. Then these rock samples were divided into 100 Ma age bins (or used in the moving average calculation – Fig. 2) and the total probability for each of the five categories was summed across each age bin. These summed probabilities were grouped into ‘reworked’ and ‘juvenile’ categories by adding the probabilities of a given rock being derived from a ‘sediment’, ‘felsic’, or ‘intermediate’ source categories together (reworked) and adding ‘mafic’ and ‘ultramafic’ categories together to get ‘juvenile’. These final summed probabilities were then normalised to calculate the reworking fraction of that age bin.

Sensitivity Testing in Relation to Calculated Crustal Growth Curves

Importantly, our calculation is not dependent on the number of preserved rock samples through time, only on the distribution of rocks derived from juvenile sources and those derived from continental reworking. This is shown in Figure 3 by a calculation of continental growth rates using a whole-rock database that includes a modelled Mesoarchean-Hadean continental crust.

To perform our modelled Mesoarchean-Hadean crust calculation, we modelled >3.2 Ga continental rocks as equivalent in number and distribution to those preserved from the Neoproterozoic – of which there is a globally-

representative set of samples in the (Gard *et al.*, 2019) database. Figure S-7 shows the number of samples over time used for this paper.

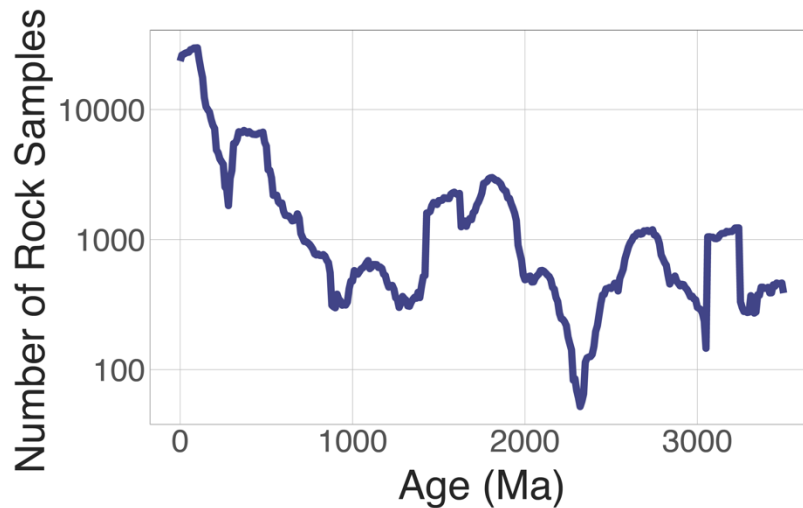


Figure S-7 The number of samples in the whole-rock database, calculated in a moving window that replicates the calculation for the reworking index shown in Fig. 3 of the manuscript.

Figure 3 of the main text shows the continental growth curve calculated by correcting for continental reworking using a synthetic Archean-Hadean rock record, and Supplementary Table S-2 to S-4 show the calculations that yield curves plotted in Figure 3. However, in order to fully test the sensitivity of our approach, we show two more calculations. Both of these calculations aim to test the influence of crustal reworking on the continental growth rates calculated here. First, we aimed to determine how much influence the calculated reworking rates had on our derived crustal growth rates. For instance, our Theta whole-rock reworking calculation clearly has the potential to be biased towards more reworking, as evidenced by our naïve Bayesian classifier applied to the Kohistan arc batholith (Fig. S-5) which showed low probabilities of ‘reworked crust’ in this location – well known to be comprised of juvenile crustal packages (Jagoutz, 2014).

To test the influence of potential systematic biases in our reworking calculation, we performed the same suite of crustal growth rate calculations using, instead of our calculated reworking rate (Fig. 2), extreme choices for uniform crustal reworking rates of 99% and 1% (0.99 and 0.01) across the entire span of geologic time. These extreme reworking rates were multiplied back onto the Hf-isotope database as in Figure S-1. Figure S-8 shows the results of these calculations and their influence on the resulting crustal growth curves. The left panel shows the reworking fractions used in our calculation, and the right panel shows the calculated growth rates using the three reworking fractions, 0.01 (constant through time), 0.99 (constant through time), and the Theta value. As shown in the right panel, our calculation is relatively insensitive to the raw reworking value used through time. In other words, even if our Theta value reworking metric was systematically biased – for instance overestimating reworking as in the Kohistan example – it would not substantially affect our calculated growth rates.

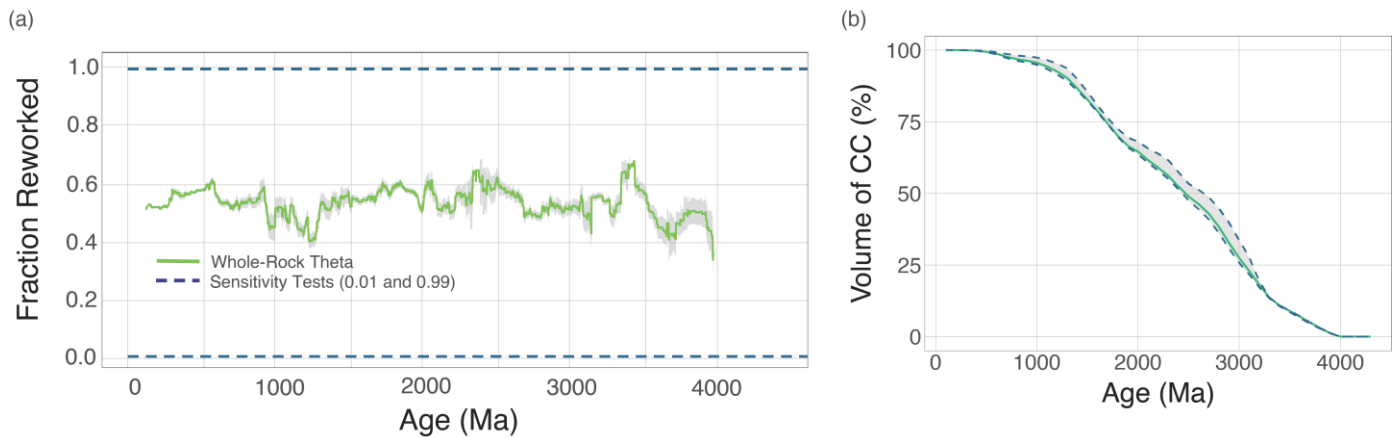


Figure S-8 A sensitivity test showing the effect of systematic bias in reworking propagated onto our crustal growth curves. **(a)** shows the crustal reworking fraction as determined by the whole rock record, and synthetic reworking estimates of 0.01 and 0.99. **(b)** shows the results of these reworking estimates propagated through the crustal growth curve. Even in the instance of an extreme bias (0.99 reworking through time) there is no significant change in the crustal growth rate calculated here (right panel where the y-axis shows the fraction of continental crust normalised to present). Therefore our calculation is relatively insensitive to systematic biases in crustal reworking.

Secondly, we test the sensitivity of our crustal growth rate calculation to temporal biases in the theta calculation. To do this, we again perform the same calculation with an extreme set of hypothetical reworking estimates. Figure S-9 shows the results of this test. First, we calculated crustal growth rates by assuming that the Archean (>2.5 Ga) had a low reworking rate of 0.10 and the post-Archean had a higher reworking rate of 0.80. This calculation is shown by the purple curve in Fig. S-9. Next we calculated the crustal growth rate for a hypothetical reworking rate where the Archean had a higher reworking rate (0.80) and the post-Archean was lower (0.10). There is significant offset between these two curves (Fig. S-9). However, our Theta reworking index shows no signs for a systematic bias across the Archean, or any other, geologic boundary in Earth history. This is contrary to the zircon $\delta^{18}\text{O}$ reworking tracer which, as discussed above, is a temporally biased reworking indicator and should not be used as a reliable tracer throughout Earth history.

The above tests show that our Theta reworking indicator and the resulting crustal growth curves are not dramatically affected by any systematic bias in the reworking metric (Fig. S-8), and they are only sensitive to time-varying biases which are unlikely to be present in our whole-rock based metric (Fig. S-9), contrary to the commonly used zircon based reworking filter.

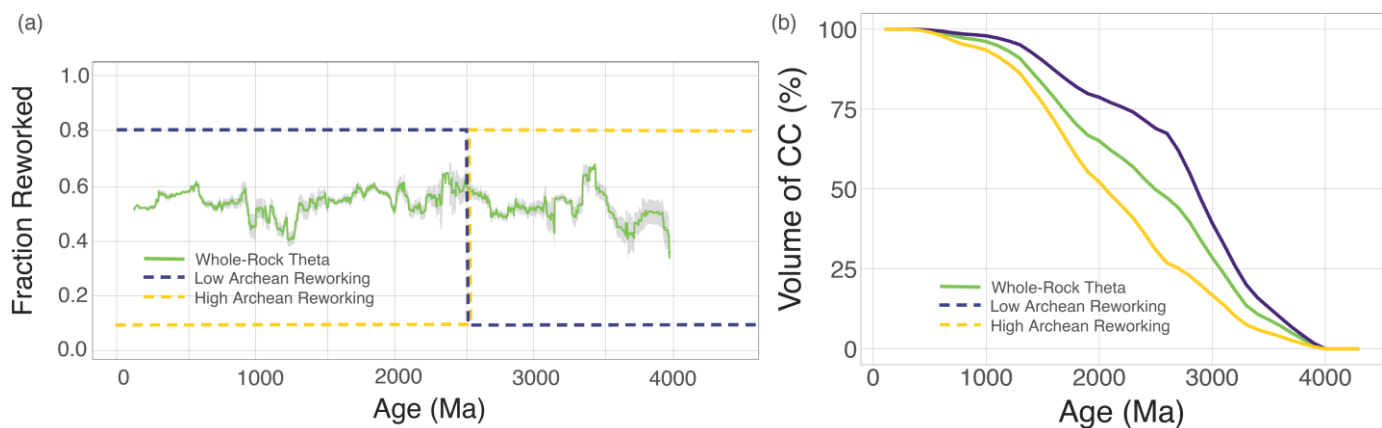


Figure S-9 A sensitivity test showing the effect of time-varying bias in reworking propagated onto our crustal growth curves. **(a)** Shows the reworking fractions through time. The purple curves show the effect of a low (0.10) Archean reworking fraction followed by a step function change to high (0.80) reworking fraction post-Archean. As shown in **(b)**, this produces a more rapid crustal growth rate followed by an inflection point in the Archean-Proterozoic boundary. Conversely, the yellow lines show the effect of high (0.80) Archean reworking followed by low post-Archean reworking (0.10). Our whole-rock Theta approach to quantifying crustal reworking shows no evidence for a time-varying bias in the reworking rate.

Uncertainty in the Mantle Age Distribution

The cratonic mantle age distribution shown in Fig. 1 is from a recently published database of cratonic lithosphere ages (Pearson *et al.*, 2021). The data plotted in Fig. 1 are the distribution of samples that were categorised as unmodified cratonic lithosphere ages. We generated uncertainties in the cumulative mantle age curve by resampling the underlying Re-depletion age (TRD) database incorporating uncertainties of ± 200 Ma for each TRD calculation. For the 913 TRD ages in the Pearson *et al.* (2021) database, we recalculated the age for each TRD by randomly selecting an age within a Gaussian uncertainty distribution. For example, for a sample with a TRD age of 2000 Ma, we would select an age randomly from a distribution with a mean of 2000 Ma and a standard deviation of 100 Ma. This was done for each sample with a TRD age in the database and a cumulative distribution was calculated. This process was repeated 100 times to estimate the range of cumulative age distributions that are possible within uncertainty (Figure S-10).

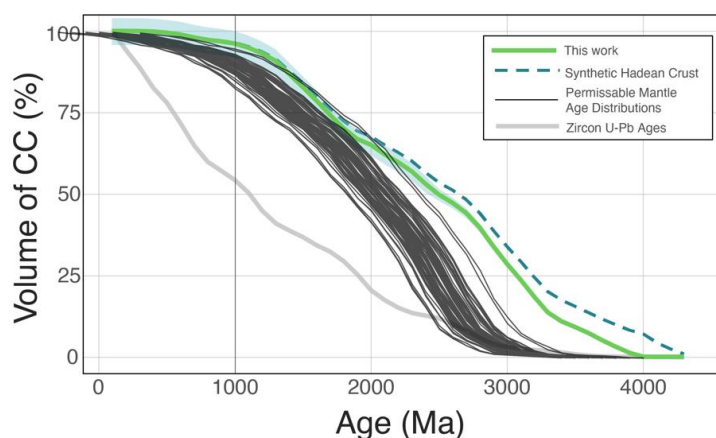


Figure S-10 Resampling of the mantle age distributions conducted to incorporate analytical and calculation uncertainty.



Implications of Alteration on Whole-Rock Reworking Signals

Whole-rock compositions, particularly those from the ancient rock record, are susceptible to chemical overprinting by metamorphism and/or weathering. While our analysis, like all compilations, relies on the original publications to obtain reliable geochemical data from relatively-well preserved rock samples, we must evaluate the impact of chemical overprinting on our whole-rock reworking estimate. Figure S-11 shows one example of this. In this analysis we calculate the reworking index for a suite of chemically altered granites from the original definition of the Chemical Alteration Index (Nesbitt and Young, 1982). The alteration signature moves data points well outside of the plotting area and as such are easily identified as altered. Any whole rock analyses in the data base that plotted well outside of the triangular field were removed as possible alteration. It is important to note that the plotting space shown in these plots are projected from other compositional space, so the actual theta value derived is dependent on other elements/oxides such as FeO in the whole rock. This is by design and calibrated to the mineralogy of the sample (Bonin *et al.*, 2020).

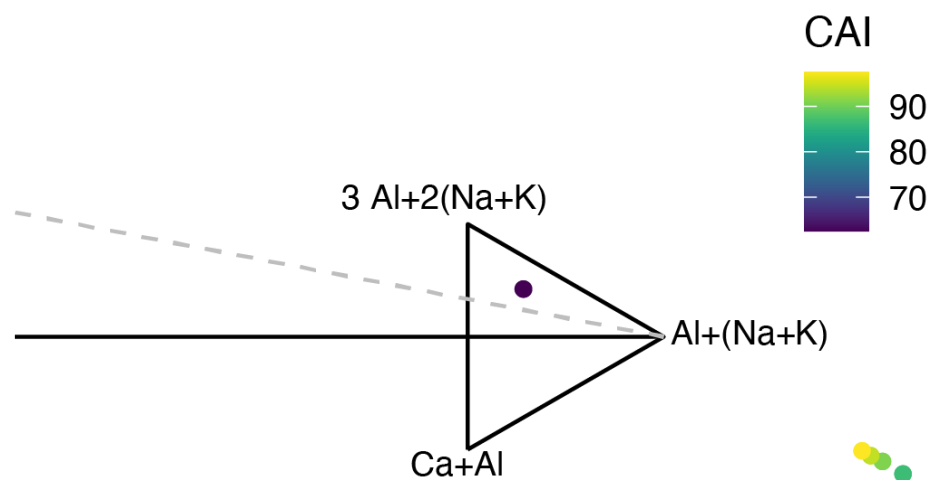


Figure S-11 Altered granite samples projected in the whole-rock reworking plotting space. The dark data point is the unaltered granite sample, while the altered samples are shown in the lower right outside of the plotting area, where CAI is the Chemical Alteration Index and is a metric used to track chemical weathering.

Supplementary Tables

The supplementary tables outline the various models of crustal growth rate, with calculations embedded. Each sheet in the downloadable Excel file represents a different crustal growth rate calculation using various reworking metrics.

Table S-1 Crustal reworking fraction through time calculated in this work and plotted in figures throughout this manuscript.

Table S-2 Dhuime *et al.* (2012) crustal growth rate calculations reproduced for clarity.

Table S-3 Whole-rock based crustal growth rates calculated in this work.

Table S-4 Crustal growth rate models using a synthetic Hadean crust model to test the sensitivity of our calculations.

Tables S-1 through S-4 (.xlsx) are available for download from the online version of this article at <https://doi.org/10.7185/geochemlet.2324>.



Supplementary Information References

- Ackerson, M., Trail, D., Buettner, J. (2021) Emergence of peraluminous crustal magmas and implications for the early Earth. *Geochemical Perspectives Letters* 17, 50–54. <https://doi.org/10.7185/geochemlet.2114>
- Arndt, N., Leshar, M.C., Barnes, S.J. (2008) *Komatiite*. Cambridge University Press. 487p <https://doi.org/10.1017/CBO9780511535550>
- Belousova, E.A., Kostitsyn, Y.A., Griffin, W.L., Begg, G.C., O'Reilly, S.Y., Pearson, N.J. (2010) The growth of the continental crust: Constraints from zircon Hf-isotope data. *Lithos* 119, 457–466. <https://doi.org/10.1016/j.lithos.2010.07.024>
- Bindeman, I.N., Bekker, A., Zakharov, D.O. (2016) Oxygen isotope perspective on crustal evolution on early Earth: A record of Precambrian shales with emphasis on Paleoproterozoic glaciations and Great Oxygenation Event. *Earth and Planetary Science letters* 437, 101–113. <https://doi.org/10.1016/j.epsl.2015.12.029>
- Bindeman, I.N., Zakharov, D.O., Palandri, J., Greber, N.D., Dauphas, N., Retallack, G.J., Hofmann, A., Lackey, J.S., Bekker, A. (2018) Rapid emergence of subaerial landmasses and onset of a modern hydrologic cycle 2.5 billion years ago. *Nature* 557, 545–548. <https://doi.org/10.1038/s41586-018-0131-1>
- Bonin, B., Janoušek, V., Moyen, J.-F. (2020) Chemical variation, modal composition and classification of granitoids. *Geological Society, London, Special Publications* 491, 9–51. <https://doi.org/10.1144/SP491-2019-138>
- Bucholz, C.E., Jagoutz, O., Jagoutz, O.E., VanTongeren, J.A., Setera, J., Wang, Z. (2017) Oxygen isotope trajectories of crystallizing melts: Insights from modeling and the plutonic record. *Geochimica et Cosmochimica Acta* 207, 154–184. <https://doi.org/10.1016/j.gca.2017.03.027>
- Bucholz, C.E., Spencer, C.J. (2019) Strongly Peraluminous Granites across the Archean–Proterozoic Transition. *Journal of Petrology* 60, 1299–1348. <https://doi.org/10.1093/petrology/egz033>
- Chappell, B.W., White, A.J.R. (2001) Two contrasting granite types: 25 years later. *Australian Journal of Earth Sciences* 48, 489–499. <https://doi.org/10.1046/j.1440-0952.2001.00882.x>
- Collins, W.J. (1996) Lachlan Fold Belt granitoids: products of three-component mixing. *Earth and Environmental Science Transactions of the Royal Society of Edinburgh* 87, 171–181. <https://doi.org/10.1017/S0263593300006581>
- Dhuime, B., Hawkesworth, C.J., Cawood, P.A., Storey, C.D. (2012) A Change in the Geodynamics of Continental Growth 3 Billion Years Ago. *Science* 335, 1334–1336. <https://doi.org/10.1126/science.1216066>
- Dhuime, B., Hawkesworth, C.J., Delavault, H., Cawood, P.A. (2017) Continental growth seen through the sedimentary record. *Sedimentary Geology* 357, 16–32. <https://doi.org/10.1016/j.sedgeo.2017.06.001>
- Dong, J., Fischer, R.A., Stixrude, L.P., Lithgow-Bertelloni, C.R. (2021) Constraining the Volume of Earth's Early Oceans With a Temperature-Dependent Mantle Water Storage Capacity Model. *AGU Advances* 2, e2020AV000323. <https://doi.org/10.1029/2020AV000323>
- Frost, B.R., Barnes, C.G., Collins, W.J., Arculus, R.J., Ellis, D.J., Frost, C.D. (2001) A Geochemical Classification for Granitic Rocks. *Journal of Petrology* 42, 2033–2048. <https://doi.org/10.1093/petrology/42.11.2033>



- Gard, M., Hasterok, D., Halpin, J.A. (2019) Global whole-rock geochemical database compilation. *Earth System Science Data* 11, 1553–1566. <https://doi.org/10.5194/essd-11-1553-2019>
- Gray, C.M. (1984) An isotopic mixing model for the origin of granitic rocks in southeastern Australia. *Earth and Planetary Science Letters* 70, 47–60. [https://doi.org/10.1016/0012-821X\(84\)90208-5](https://doi.org/10.1016/0012-821X(84)90208-5)
- Grove, T.L., Parman, S.W. (2004) Thermal evolution of the Earth as recorded by komatiites. *Earth and Planetary Science Letters* 219, 173–187. [https://doi.org/10.1016/S0012-821X\(04\)00002-0](https://doi.org/10.1016/S0012-821X(04)00002-0)
- Jagoutz, O. (2014) Arc crustal differentiation mechanisms. *Earth and Planetary Science Letters* 396, 267–277. <https://doi.org/10.1016/j.epsl.2014.03.060>
- Kemp, A.I.S., Hawkesworth, C.J., Foster, G.L., Paterson, B.A., Woodhead, J.D., Hergt, J.M., Gray, C.M., Whitehouse, M.J. (2007) Magmatic and crustal differentiation history of granitic rocks from Hf-O isotopes in zircon. *Science* 315, 980–983. <https://doi.org/10.1126/science.1136154>
- Korenaga, J. (2018) Estimating the formation age distribution of continental crust by unmixing zircon ages. *Earth and Planetary Science Letters* 482, 388–395. <https://doi.org/10.1016/j.epsl.2017.11.039>
- Kump, L.R., Barley, M.E. (2007) Increased subaerial volcanism and the rise of atmospheric oxygen 2.5 billion years ago. *Nature* 448, 1033–1036. <https://doi.org/10.1038/nature06058>
- Laurent, O., Martin, H., Martin, H., Moyen, J.F., Moyen, J.-F., Doucelance, R., Doucelance, R. (2014) The diversity and evolution of late-Archean granitoids: Evidence for the onset of “modern-style” plate tectonics between 3.0 and 2.5Ga. *Lithos* 205, 1–82. <https://doi.org/10.1016/j.lithos.2014.06.012>
- Martin, H. (1986) Effect of steeper Archean geothermal gradient on geochemistry of subduction-zone magmas. *Geology* 14, 753–756. [https://doi.org/10.1130/0091-7613\(1986\)14<753:EOSAGG>2.0.CO;2](https://doi.org/10.1130/0091-7613(1986)14<753:EOSAGG>2.0.CO;2)
- Moyen, J.-F., Martin, H. (2012) Forty years of TTG research. *Lithos* 148, 312–336. <https://doi.org/10.1016/j.lithos.2012.06.010>
- Nesbitt, H.W., Young, G.M. (1982) Early Proterozoic climates and plate motions inferred from major element chemistry of lutites. *Nature*. <https://doi.org/10.1038/299715a0>
- Pearson, D.G., Scott, J.M., Liu, J., Schaeffer, A., Wang, L.H., van Hunen, J., Szilas, K., Chacko, T., Kelemen, P.B. (2021) Deep continental roots and cratons. *Nature* 596, 199–210. <https://doi.org/10.1038/s41586-021-03600-5>
- Reimink, J.R., Davies, J.H.F.L., Ielpi, A. (2021) Global zircon analysis records a gradual rise of continental crust throughout the Neoproterozoic. *Earth and Planetary Science Letters* 554, 116654. <https://doi.org/10.1016/j.epsl.2020.116654>
- Roberts, N.M.W., Spencer, C.J. (2015) The zircon archive of continent formation through time. *Geological Society, London, Special Publications* 389, 197–225. <https://doi.org/10.1144/SP389.14>
- Shand, S.J. (1943) *Eruptive rocks: Their genesis, composition, and classification, with a chapter on meteorites*. J. Wiley & sons, Incorporated.
- Walter, M.J. (1998) Melting of Garnet Peridotite and the Origin of Komatiite and Depleted Lithosphere. *Journal of Petrology* 39, 29–60. <https://doi.org/10.1093/etroj/39.1.29>

